

Supplemental Methods

RNA isolation from bulk bone marrow suspensions

RNA was isolated and processed as previously described.¹ Approximately 100 ng per sample of RNA extracted from bulk bone marrow (BM) aspirates were analyzed on the nCounter FLEX analysis system (NanoString Technologies, Seattle, WA) using the PanCancer IO 360 panel (for research use only and not for use in diagnostic procedures). The reporter probe counts, i.e., the number of times the color-coded barcode for that gene is detected, were tabulated in a comma separated value format for data analysis with the nSolver software package (version 4.0.62) and nSolver Advanced Analysis module (version 2.0.115; NanoString Technologies). The captured transcript counts were normalized to the geometric mean of the housekeeping reference genes included in the assay and the code set's internal positive controls. The relative abundance of immune cell types and immuno-oncology biological signatures were computed as previously published (**Supplemental Table 1**).^{2,3}

Data sources for *in silico* analyses

The Cancer Genome Atlas (TCGA) series consisted of RNA-sequencing data (Illumina HiSeq2000) from 147 adult AML patients with complete cytogenetic, immunophenotypic and clinical annotation who were enrolled on Cancer and Leukemia Group B treatment protocols 8525, 8923, 9621, 9720, 10201 and 19808. Fourteen patients had a documented *TP53* mutation. RNA and clinical data were retrieved from cBioPortal for Cancer Genomics (<https://www.cbioportal.org/>).⁴ Level 3 RSEM-normalized RNASeqV2 data was downloaded from TCGA and log₂-transformed prior to analysis. No further pre-processing was applied. For mRNA expression data, cBioPortal for Cancer Genomics computes the relative expression of an individual gene and tumor specimen to the gene's distribution in all samples that are diploid for the gene in question. The returned value (z-score) indicates the number of standard deviations

away from the mean of expression in all other tumor samples. To ensure high stringency, a z-score threshold of ± 2.0 was used in all analyses. Patients had a median age of 60 years, 54% were male, with 12%, 65% and 22% classified as favorable, intermediate and adverse risk, respectively, based on 2017 European Leukemia-Net (ELN) risk stratification by genetics (**Table 1**). One hundred thirteen patients (77%) were reported as having received “7+3” cytotoxic induction chemotherapy. The remaining patients were treated with adjunctive therapy in addition to “7+3” or with HMAs.

AML cell lines

For *in vitro* modeling experiments, commercial AML cell lines that harbor a missense (R248Q; Kasumi-1 cells; ATCC CRL-2724) and a truncating mutation of *TP53* (KG-1 cells; ATCC CRL-246), respectively, were selected. Kasumi-1 cells were cultured in RPMI (Lonza, Basel, Switzerland) supplemented with 20% fetal bovine serum (FBS; HyClone; GE Healthcare Life Sciences, Pittsburgh, PA, USA) and 2 mM L-glutamine (Lonza). KG-1 cells were cultured with IMDM containing 25 mM HEPES and L-glutamine +20% FBS. Cells were seeded at 1.5×10^6 per well in a 6-well plate with or without 100 ng/mL IFN- γ (R&D systems, Bio-Techne Ltd., UK) and were harvested at pre-defined timepoints for further processing. In selected mechanistic experiments, cells were pre-treated for 24 hours either with a methylated derivative of Prima-1 (Prima-1^{MET}; 25 μ M; TOCRIS, Abingdon, UK), a mutant *TP53* reactivator, or with nutlin-3, an MDM2 inhibitor (5 μ M; Sigma-Aldrich, St. Louis, MI), before IFN- γ stimulation. Cell lysates of AML cell lines were used for the integrated measurement of mRNA, protein and single nucleotide variants (SNV) with the nCounter Vantage 3D Heme Panel (NanoString Technologies), as per manufacturer's protocol. Cell lines HuT-78 (mature T cells from a case of Sezary syndrome) and CCRF-CEM (T cell acute lymphoblastic leukemia) with known mutations in key cancer drivers were used as controls.

Enumeration of immune cell fractions in gene expression datasets

CIBERSORT was used to deconvolute TCGA-AML RNA sequencing data and to quantify immune cell types of interest in the AML tumor microenvironment.⁵ CIBERSORT relies on a signature matrix (LM22) consisting of 547 genes that distinguish 22 functionally defined human hematopoietic cell types, including T-cell subsets, naïve and memory B cells, plasma cells, NK cells and myeloid cell subsets.

Single cell RNA-sequencing profiles of BM samples from healthy donors (n=4) and AML patients (n=16, 3 with mutations of *TP53*) were downloaded from Gene Expression Omnibus (GSE116256).⁶

Gene ontology (GO) and gene set enrichment analysis (GSEA)

For the gene list submitted to metascape.org, GO pathway and process enrichment analyses are carried out using all genes in the genome as the enrichment background.⁷ To account for multiple hypothesis testing, we used a false discovery rate set at 01%. Terms with a *P* value < 0.01, a minimum count of 3, and an enrichment factor >1.5 (defined as the ratio between the observed counts and the counts expected by chance) are collected and grouped into clusters based on their membership similarities. GSEA was performed using the GSEA software v.3.0 (Broad Institute, Cambridge, USA).⁸ Two *TP53* Pathway Gene Sets (n=200 genes involved in *TP53* pathways and networks (M5939) and n=172 genes upregulated in National Cancer Institute (NCI)-60 cancer cell lines with mutated *TP53* (M2698)) were downloaded from the Molecular Signature Database (MSigDB). The analysis of functional protein association networks was performed using STRING (<https://string-db.org/>).

Flow cytometry

AML cell lines (0.5×10^6) were aliquoted into 12x75mm tubes and were incubated with 5µL Human FcR Blocking Reagent (Miltenyi Biotec, Bergisch Gladbach, Germany), fluorochrome-conjugated

monoclonal antibodies against IFN- γ receptor I (CD119; clone GIR-94), PD-L1 (clone 29E.2A3) and HLA-A,B,C (clone W6/32; BioLegend, San Diego, CA, USA), and LIVE/DEAD fixable viability dyes (ThermoFisher Scientific, Waltham, MA, USA) for 30 minutes at 4°C, protected from light. Cells were finally re-suspended in 350 μ L PBS and were run through a Gallios flow cytometer (Beckman Coulter, High Wycombe, UK). Data were analyzed with the Kaluza software package, v1.3 (Beckman Coulter).

Cryopreserved peripheral blood or BM mononuclear cells were thawed, washed in PBS and stained 15 minutes at room temperature with a LIVE/DEAD Fixable Blue Dead Cell Stain kit (Invitrogen, Carlsbad, CA). Cells were then washed in PBS supplemented with 0.5% bovine serum albumin and 2 mM EDTA and incubated for 10 min at room temperature with human Fc Block (BD Biosciences; San Jose, CA). Pre-titrated saturating dilutions of fluorochrome-labeled antibodies (**Supplemental Table 10**) were added and cells incubated for 30 min at room temperature. Intracellular staining for Ki-67 and Granzyme B was performed using a transcription factor staining buffer set (Thermo Fisher Scientific, Waltham, MA) according to the manufacturer's instructions. Fluorescence-minus-one controls were used to assess background fluorescence intensity and set gates for negative populations. Samples were analyzed on a Gallios or ZE5 (Bio-Rad, Hercules, CA) flow cytometer. Single stain compensation controls were obtained using UltraComp eBeads (Thermo Fisher Scientific) and data were analyzed using FlowJo software (TreeStar, Ashland, OR).

Supplemental Tables

Supplemental Table 1: Immune cell type-specific and biological activity mRNA scores computed in this study.

Biological activity scores	Immune cell type-specific scores	Immune checkpoints
APM	B cells	B7-H3
APM loss	CD45	CTLA4
Apoptosis	CD8 T cells	IDO1
ARG1	Cytotoxic cells	PD1
Cytotoxicity	DCs	PDL1
Exhausted CD8 cells	Endothelial cells	PDL2
Glycolytic activity	Lymphoid cells	TIGIT
Hypoxia	Macrophages	
IFN- γ	Mast cells	
IFN downstream	Myeloid cells	
IL10	Neutrophils	
Immunoproteasome	CD56 ^{dim} NK cells	
Inflammatory chemokines	NK cells	
MAGEs	T cells	
MHC2	Th1 cells	
MMR loss	Treg cells	
Myeloid inflammation		
NOS2		
Proliferation		
Stroma		
TGF- β		
TIS		

Legend: APM = antigen processing machinery; ARG1 = arginase 1; IFN = interferon; MHC2 = major histocompatibility class II; MMR = mismatch repair; NOS2 = nitric oxide 2; TGF = transforming growth factor; TIS = tumor inflammation signature; DCs = dendritic cells; NK = natural killer; Th1 = T helper type 1.

Supplemental Table 2: Somatic *TP53* mutations in the TCGA-AML cohort

Sample ID	Protein change	Mutation type*
TCGA-AB-2943-03	R273C	Missense
TCGA-AB-2935-03	R248Q	Missense
TCGA-AB-2813-03	C176Y	Missense
TCGA-AB-2938-03	H179R	Missense
TCGA-AB-2938-03	R342Efs*3	Frameshift
TCGA-AB-2908-03	C141W	Missense
TCGA-AB-2908-03	Q317*	Nonsense
TCGA-AB-2885-03	H193Y	Missense
TCGA-AB-2829-03	R280G	Missense
TCGA-AB-2829-03	X225_splice	Splice site
TCGA-AB-2904-03	R337C	Missense
TCGA-AB-2952-03	E286G	Missense
TCGA-AB-2941-03	I195S	Missense
TCGA-AB-2878-03	V173*	Frameshift
TCGA-AB-2878-03	S215G	Missense
TCGA-AB-2820-03	P223Rfs*4	Frameshift
TCGA-AB-2860-03	M40Lfs*7	Frameshift
TCGA-AB-2838-03	T125=	Splice site
TCGA-AB-2868-03	X126_splice	Splice site
TCGA-AB-2857-03	X10_splice	Splice site

Legend: *IARC *TP53* Database. Two different *TP53* mutations were identified in 4 patients from this series (orange highlight).

Supplemental Table 3: List of genes used for gene set enrichment analysis (GSEA)⁸ in TCGA AML cases with *TP53* mutations.

Senescence	Immune senescence	T-cell exhaustion
<i>ABL1</i>	<i>B3GAT1</i>	<i>PDCD1</i>
<i>CD44</i>	<i>KIR2DL1</i>	<i>HAVCR2</i>
<i>CDKN1A</i>	<i>KLRG1</i>	<i>CD244</i>
<i>EGR1</i>	<i>KLRC1</i>	<i>BTLA</i>
<i>ETS1</i>	<i>KLRC3</i>	<i>CTLA4</i>
<i>FN1</i>	<i>KLRD1</i>	<i>CD160</i>
<i>HRAS</i>	<i>KLRF1</i>	<i>TIGIT</i>
<i>IGF1R</i>		<i>LAG3</i>
<i>IRF5</i>		<i>TOX</i>
<i>PLAU</i>		<i>TOX2</i>
<i>PRKCD</i>		<i>NR4A1</i>
<i>SERPINB2</i>		<i>NR4A2</i>
		<i>NR4A3</i>

Supplemental Table 4: Somatic *TP53* mutations in SAL-AML cases (n=40 patients).

Subject ID	Protein change	Mutation type*
32-2-001	G360E	N.A.
02-1-053	R181C	Missense
03-1-006	T211I	Missense
03-1-120	P151S	Missense
03-1-166	H178P	Missense
03-1-174	[STOP] AA	Frameshift
03-1-225	T125M	Missense
08-1-024	R175H	Missense
09-1-051	K132T	Missense
09-1-077	C238Y	Missense
09-1-114	V272M	Missense
09-1-130	R175G	Missense
09-1-143	R248Q	Missense
09-1-222	R248Q	Missense
10-1-012	E286K	Missense
10-1-024	R248W	Missense
10-1-082	I195T	Missense
12-1-002	H179Y	Missense
15-1-018	[STOP] AA 344	Frameshift
15-1-025	[STOP] AA 125	Frameshift
16-1-031	R280G	Missense
23-1-026	I195N	Missense
28-1-020	P278R	Missense
29-1-010	M237K	Missense
30-1-008	M246V	Missense
30-1-008	R283C	Missense
30-1-130	Y → [STOP]	Frameshift
33-1-003	H193R	Missense
35-1-022	F270C	Missense
37-1-006	R283C	Missense
39-1-027	[STOP] AA 169	Frameshift
39-1-027	Y220C	Missense
007-001-115	R283QR	N.A.
036-006-154	N235S	Missense
046-021-326	V216M	Missense
R-S-014-154-00RH	P151T	Missense
R-S-030-140-CC3U	R273H	Missense
R-S-039-025-ECR7	E286G	Missense
R-S-052-018-N3CL	V272M	Missense
R-S-054-137-44VL	G245V	Missense
R-S-067-024-VSLZ	N235S	Missense
R-S-030-176-ZZQH	C275Y	Missense

Legend: *IARC *TP53* Database. Two different *TP53* mutations were identified in 2 patients from this series (green highlight).

Supplemental Table 5: Top differentially expressed genes (ranked by log₂ fold change) between patients with *TP53* mutated and *TP53* wild type AML. Results were filtered to include only those genes that displayed ≥1.5-fold changes in expression and had passed a test for statistical significance ($P < 0.01$).

Gene Id	Log2 fold change	P value
<i>Up in TP53 mutated AML</i>		
THBD	3.28	2.88×10 ⁻¹⁰
IL33	2.67	4.31×10 ⁻⁶
CCL3/L1	2.61	1.44×10 ⁻⁶
IL6	2.32	0.0001396
CXCL8	2.25	2.27×10 ⁻⁵
RIPK2	2.15	9.04×10 ⁻¹³
CCL2	2.12	0.0283116
THBS1	2.10	0.0061577
CXCL1	2.09	0.0001883
CSF1	2.01	2.65×10 ⁻⁵
MYCT1	1.97	9.35×10 ⁻⁶
OASL	1.92	0.0002112
PTGER4	1.92	2.37×10 ⁻¹⁰
CXCL2	1.82	2.65×10 ⁻⁵
BBC3	1.81	1.64×10 ⁻⁶
DUSP5	1.77	1.48×10 ⁻⁷
IFNG	1.73	0.000511
FCAR	1.71	0.001586
<i>Up in TP53 wild type AML</i>		
CD2	-1.61	3.91×10 ⁻⁸
CD79A	-1.73	0.0003015
CD79B	-1.76	0.0006327
GIMAP6	-1.88	6.53×10 ⁻⁵
CCR2	-1.89	3.28×10 ⁻⁵
PRF1	-1.94	0.0003822
FAM30A	-1.97	0.0250546
NT5E	-2.01	9.74×10 ⁻⁷
ITGB3	-2.09	1.07×10 ⁻⁶
CD19	-2.20	1.49×10 ⁻⁵
CXCR2	-2.32	2.92×10 ⁻⁵
MS4A1	-3.40	2.25×10 ⁻⁹
GBP1	-3.57	1.38×10 ⁻⁶
VTCN1	-3.88	6.96×10 ⁻²²
MARCO	-3.96	2.30×10 ⁻⁷
CX3CR1	-4.72	2.24×10 ⁻⁸

Supplemental Table 6: Gene ontologies (GO) and KEGG pathways captured by differentially expressed (DE) genes between patients with *TP53* mutated and *TP53* wild type AML. FDR = false discovery rate.

GO term	Description	Count in gene set	FDR
GO:0006955	Immune response	21 of 1560	2.94×10^{-15}
GO:0032101	Regulation of response to external stimulus	17 of 732	3.21×10^{-15}
GO:0071345	Cellular response to cytokine stimulus	18 of 953	4.67×10^{-15}
GO:0006952	Defense response	19 of 1234	9.97×10^{-15}
GO:0032103	Positive regulation of response to external stimulus	13 of 291	1.18×10^{-14}
GO:0002376	Immune system process	22 of 2370	7.55×10^{-14}
GO:0006950	Response to stress	24 of 3267	8.40×10^{-14}
GO:0006954	Inflammatory response	14 of 482	8.99×10^{-14}
GO:0019221	Cytokine-mediated signaling pathway	15 of 655	1.55×10^{-13}
Pathway	Description	Count in gene set	FDR
hsa04060	Cytokine-cytokine receptor interaction	9 of 263	5.56×10^{-9}
hsa05323	Rheumatoid arthritis	6 of 84	6.37×10^{-8}
hsa04657	IL-17 signaling pathway	6 of 92	8.02×10^{-8}
hsa04621	NOD-like receptor signaling pathway	6 of 166	1.56×10^{-6}
hsa04668	TNF signaling pathway	5 of 108	4.16×10^{-6}
hsa05200	Pathways in cancer	7 of 515	4.09×10^{-5}
hsa04151	PI3K-Akt signaling pathway	5 of 348	0.00056
hsa04062	Chemokine signaling pathway	4 of 181	0.00056
hsa04659	Th17 cell differentiation	3 of 102	0.0017

Supplemental Table 7: Top differentially expressed genes/proteins (ranked by log₂ fold change) between KG-1 (truncating *TP53* mutation) and Kasumi-1 AML cells (missense *TP53* mutation). Results were filtered to include only those genes that displayed ≥1.7-fold changes in expression and had passed a test for statistical significance ($P < 0.01$).

Gene Id	Log2 fold change	P value
<i>Up in Kasumi-1 cells</i>		
TP53 protein	10.0	0.00029
FYN-mRNA	5.56	0.00084
DNMT3A-mRNA	2.35	5.67×10 ⁻⁵
CSF3R-mRNA	2.32	4.43×10 ⁻⁵
DDIT3-mRNA	2.16	0.00085
KIT-mRNA	2.08	0.00014
CBL-mRNA	1.89	3.16×10 ⁻⁶
FOXO1-mRNA	1.83	0.0051
TP53-mRNA	1.73	0.0079
STAT6-mRNA	1.70	8.54×10 ⁻⁶
CDKN2A-mRNA	1.70	0.00021
<i>Up in KG-1 cells</i>		
EIF4E-mRNA	-1.81	0.00029
IFI16-mRNA	-1.91	1.42×10 ⁻⁵
CHEK1-mRNA	-1.96	0.0071
NLRC5-mRNA	-1.99	0.00027
Iκ-Ba-protein	-2.06	0.00031
KAT6A-mRNA	-2.13	1.68×10 ⁻⁵
IRF1-mRNA	-2.19	2.18×10 ⁻⁵
RHOA-mRNA	-2.21	3.94×10 ⁻⁵
IKKβ-protein	-2.24	3.17×10 ⁻⁶
IDH1-mRNA	-2.36	8.95×10 ⁻⁵
BCL3-mRNA	-2.50	0.00034
STAT1-mRNA	-2.57	1.41×10 ⁻⁵
RARA-mRNA	-2.64	0.00041
CCND3-mRNA	-2.74	9.71×10 ⁻⁵
STAT5A-mRNA	-3.0	1.86×10 ⁻⁵
CCND2-mRNA	-3.1	6.35×10 ⁻⁵
SYK-mRNA	-3.48	2.84×10 ⁻⁶
RAC1-mRNA	-3.75	4.02×10 ⁻⁶
LYN-mRNA	-3.78	1.32×10 ⁻⁶
LCK-mRNA	-4.02	0.00285
OSM-mRNA	-4.38	0.0059
CD34-mRNA	-4.39	4.43×10 ⁻⁷
SET-mRNA	-4.71	7.37×10 ⁻⁶

MYCN-mRNA	-4.76	0.00302
PIM1-mRNA	-4.95	2.65×10^{-6}
HOXA9-mRNA	-5.24	0.00014
NF- κ B-protein	-5.33	0.0028
IKZF2-mRNA	-5.79	2.46×10^{-5}
MEIS1-mRNA	-6.99	0.0034
CIITA-mRNA	-7.10	0.00133
HGF-mRNA	-7.25	0.00118

Supplemental Table 8: Gene ontologies (GO) and KEGG pathways captured by differentially expressed (DE) genes between KG-1 (truncating *TP53* mutation and Kasumi-1 AML (missense *TP53* mutation). FDR = false discovery rate.

GO term	Description	Count in gene set	FDR
GO:0010604	Positive regulation of macromolecule metabolic process	33 of 3081	1.17×10^{-14}
GO:0005515	Protein binding	41 of 6605	5.58×10^{-14}
GO:0004672	Protein kinase activity	15 of 635	7.21×10^{-10}
GO:0016301	Kinase activity	16 of 835	1.71×10^{-9}
GO:0010604	Positive regulation of macromolecule metabolic process	33 of 3081	1.17×10^{-14}
GO:0051171	Regulation of nitrogen compound metabolic process	39 of 5827	1.39×10^{-13}
GO:0051171	Regulation of nitrogen compound metabolic process	39 of 5827	1.39×10^{-13}
GO:0002682	Regulation of immune system process	21 of 1391	3.36×10^{-11}
GO:0016310	Phosphorylation	20 of 1236	4.28×10^{-11}
Pathway	Description	Count in gene set	FDR
hsa05203	Viral carcinogenesis	15 of 183	1.16×10^{-17}
hsa05200	Pathways in cancer	18 of 515	1.80×10^{-15}
hsa04151	PI3K-Akt signaling pathway	15 of 348	4.93×10^{-14}
hsa04218	Cellular senescence	10 of 156	4.21×10^{-11}
hsa04630	JAK-STAT signaling pathway	10 of 160	4.81×10^{-11}
hsa04659	Th17 cell differentiation	8 of 102	1.10×10^{-9}
hsa05221	Acute myeloid leukemia	7 of 66	2.30×10^{-9}
hsa04115	p53 signaling pathway	7 of 68	2.61×10^{-9}
hsa04658	Th1 and Th2 cell differentiation	7 of 88	1.33×10^{-8}

Legend: The light blue shading highlights GO terms and KEGG pathways that are also captured by the differentially expressed genes between *TP53* mutated and *TP53* wild type primary BM samples (**Supplemental Table 5**).

Supplemental Table 9: Top differentially expressed (DE) genes (ranked by log₂ fold change) in KG-1 and Kasumi-1 cells treated with 25 μM Prima-1^{MET}, a TP53 reactivator, for 24 hours. Results were filtered to include only those genes that displayed ≥1.5-fold changes in expression and had passed a test for statistical significance (*P* < 0.01).

Gene Id	Log2 fold change	<i>P</i> value
<i>DE in Prima-1^{MET}-treated Kasumi-1 AML cells</i>		
FOS	5.86	6.35×10 ⁻¹²
PTGS2	4.59	2.89×10 ⁻¹³
SOCS1	4.5	7.04×10 ⁻¹³
BCL6	4.01	3.74×10 ⁻¹¹
SOCS3	3.92	3.14×10 ⁻¹²
DDIT3	3.34	5.61×10 ⁻¹³
MCL1	2.43	1.02×10 ⁻¹¹
BCL10	2.26	7.77×10 ⁻¹⁰
CCND2	-2.28	2.51×10 ⁻¹⁰
KIT	-2.29	2.88×10 ⁻¹⁴
MYC	-2.85	6.87×10 ⁻¹⁴
SPRY2	-3.85	2.24×10 ⁻⁰⁹
DUSP6	-4.59	5.27×10 ⁻¹⁵
<i>DE in Prima-1^{MET}-treated KG-1 AML cells</i>		
FOS	3.71	3.17×10 ⁻⁴
BCL6	2.24	7.39×10 ⁻⁶

Supplemental Table 10: Antibodies used for flow cytometry.

Specificity	Clone	Fluorochrome	Source
CD3	UCHT1	AF488	BD Biosciences
CD4	SK3	BV510	BD Biosciences
CD8	RPA-T8	BUV496	BD Biosciences
CD25	2A3	BV711	BD Biosciences
CD38	HIT2	BV421	BD Biosciences
CD45	HI30	BUV395	BD Biosciences
CD69	FN50	V450	BD Biosciences
CD127	RDR5	APC-eFluor780	eBioscience
Granzyme B	GB12	APC	Invitrogen
HLA-DR	G46-6	BUV661	BD Biosciences

Abbreviations: AF, Alexa Fluor; APC, allophycocyanin; BV, Brilliant Violet; BUV, Brilliant Ultraviolet; Cy, cyanine dye; PE, R-phycoerythrin.

Supplemental Figures and Figure Legends

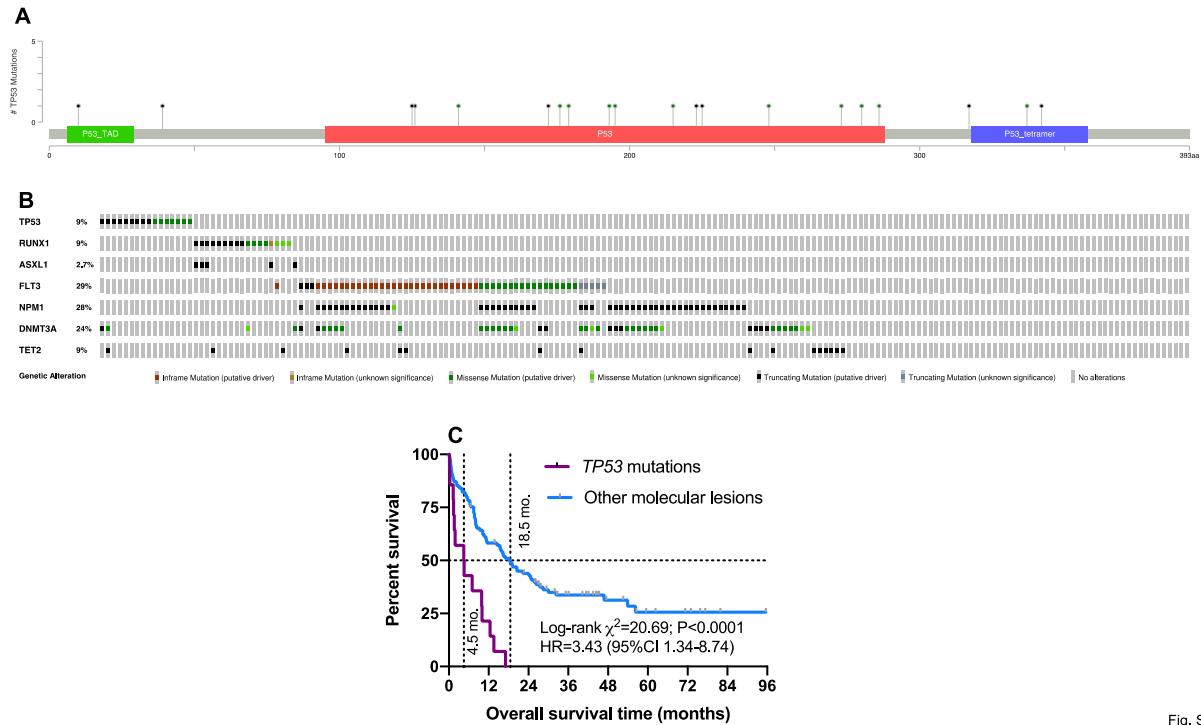


Fig. S1

Supplemental Figure 1: *TP53* mutations and patient survival in The Cancer Genome Atlas (TCGA) AML cohort. A) Lollipop plot showing *TP53* mutational data from TCGA cases (n=11 missense, n=9 truncating). TAD = transactivation domain. **B)** Co-mutation OncoPrint plot depicting prognostically relevant genes in TCGA cases with *TP53* abnormalities. Each column represents one patient for whom co-mutation data are available through cBioPortal.⁹ **C)** Kaplan-Meier estimate of overall survival in TCGA-AML cases with *TP53* mutations and other prognostic molecular lesions, as defined in the main text. Survival curves were compared using a log-rank test. HR = hazard ratio; CI = confidence interval. Dotted lines denote median survival times.

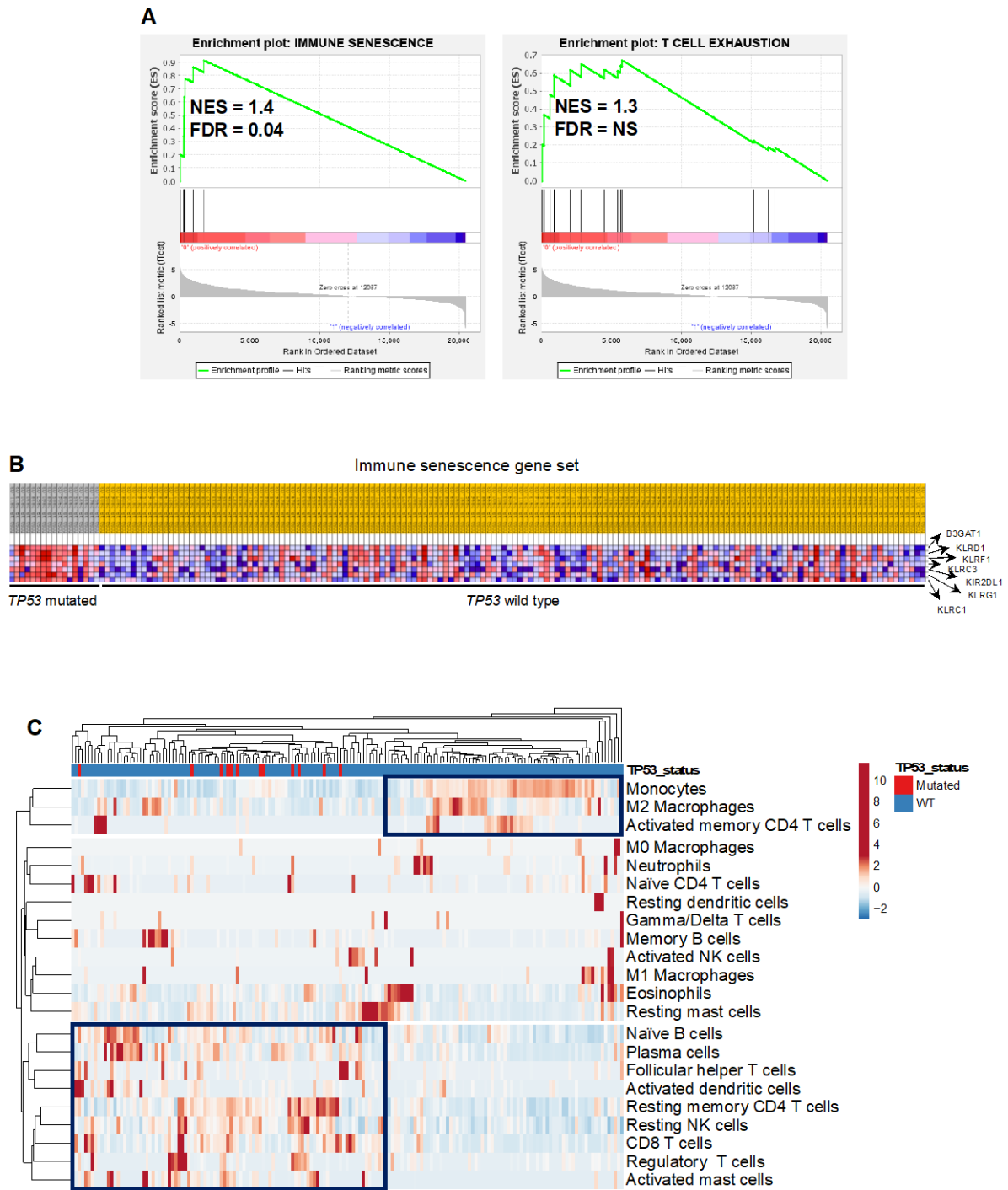
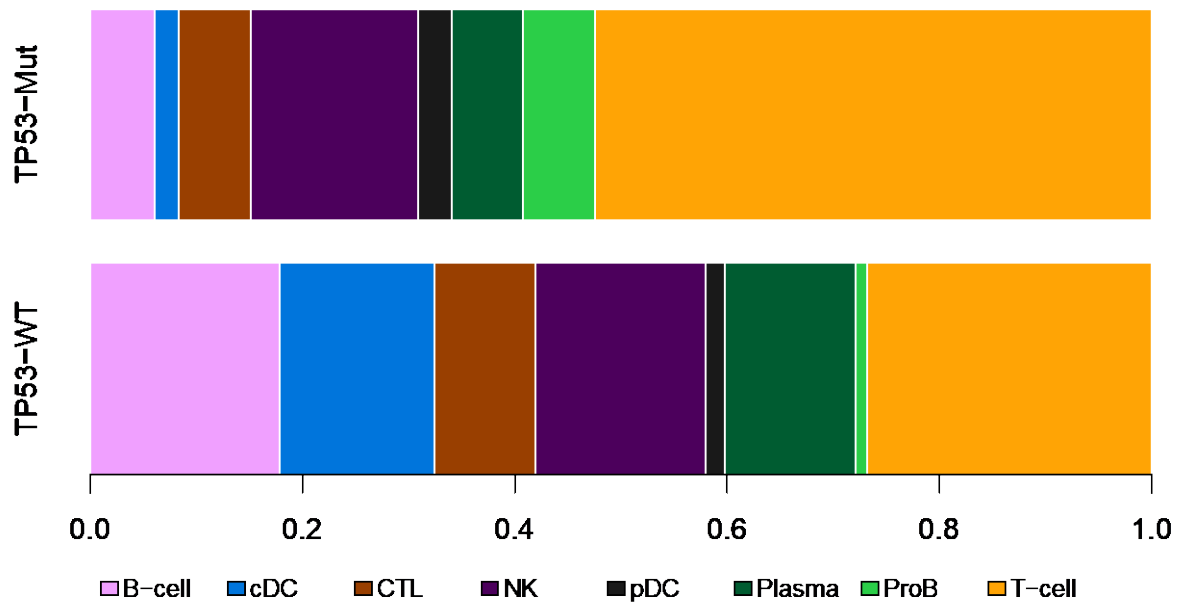


Fig. S2

Supplemental Figure 2: Gene set enrichment analysis (GSEA) and hematopoietic cell type deconvolution in *TP53* mutated cases from The Cancer Genome Atlas (TCGA) AML cohort.

A) Representative enrichment plots of select immune senescence-associated and cellular

senescence-associated gene sets overrepresented in *TP53* mutated cases from TCGA-AML. **B)** Heatmap summarizing the expression of 7 immune senescence-associated genes in *TP53* mutated and *TP53* wild type cases from TCGA-AML. Input gene lists are shown in **Supplemental Table 3**. **C)** Heat map showing the estimated frequency of 22 hematopoietic cell types as evaluated using the CIBESORT deconvolution engine in *TP53* mutated and *TP53* wild type cases from TCGA-AML.⁵ Blue boxes denote immune cell type co-expression patterns that were specifically identified in the above patient subgroups.



Supplemental Figure 3: Deconvolution of immune cell types from single cell RNA-sequencing data (GSE116256). Stacked bar plots showing the frequency of immune cell populations in BM samples from AML patients with *TP53* mutated (n=3) and *TP53*-WT (n=13) AML. In total, 944 cells from *TP53*-mutated cases and 3,100 cells from *TP53*-WT cases were used for this analysis. B-cell: mature B cells; cDC: conventional dendritic cell; CTL: cytotoxic T lymphocyte; NK: natural killer cells; pDC: plasmacytoid dendritic cells; Plasma: plasma cells; ProB: progenitor B cells; T-cell: naïve T cells.

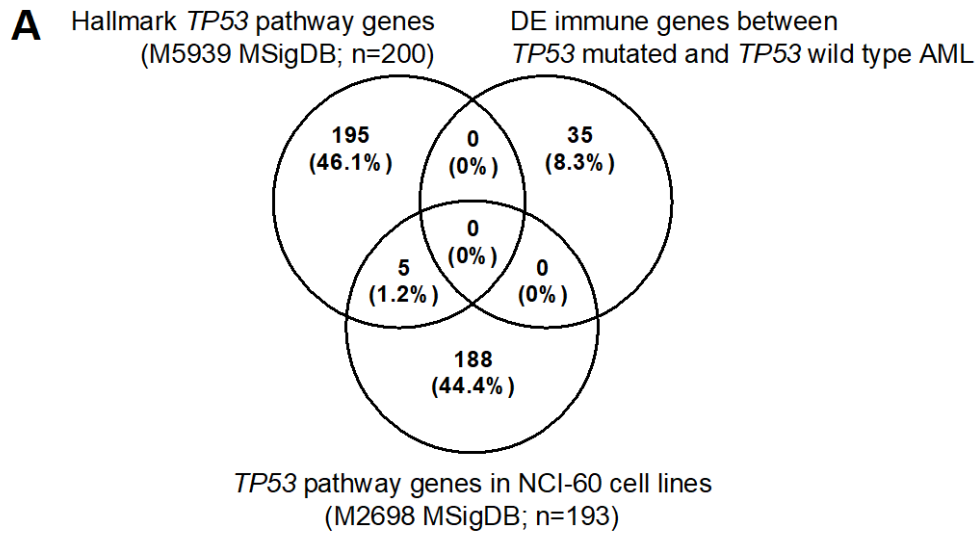


Fig. S4

Supplemental Figure 4: A) Venn diagram showing overlap between differentially expressed (DE) immune genes in patients with *TP53* mutated AML and genes previously implicated in the *TP53* pathway. The *TP53* Pathway Gene Sets (n=200 genes involved in *TP53* pathways and networks (M5939) and n=172 genes upregulated in National Cancer Institute (NCI)-60 cancer cell lines with mutated *TP53* (M2698)) were downloaded from the Molecular Signature Database (MSigDB).

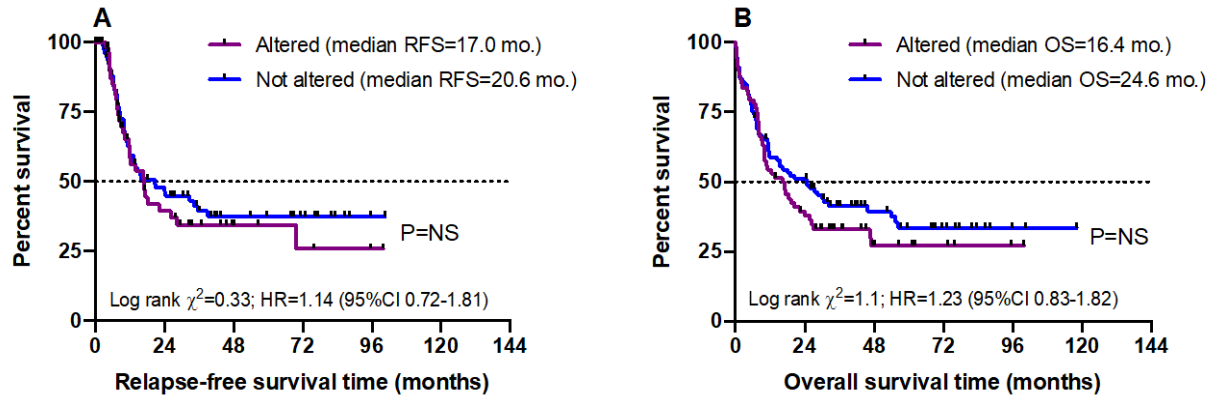


Fig. S5

Supplemental Figure 5: Downregulated genes in the *TP53* immune gene classifier do not carry prognostic significance in TCGA-AML cases. Abnormalities in the 16 downregulated immune genes in the *TP53* classifier (including mRNA upregulation, gene amplification, deep deletion and mis-sense mutations, relative to the gene's expression distribution in all profiled AML samples) in TCGA-AML cases. Data were retrieved, analyzed and visualized using cBioPortal. Abnormalities in only one gene utilized in the cBioPortal query (by default, non-synonymous mutations, fusions, amplifications and deep deletions) were sufficient to define that particular patient sample as “altered”. The Kaplan-Meier method was used to generate survival curves, which were compared using a log-rank test. RFS = relapse-free survival (**A**); OS = overall survival (**B**); HR = hazard ratio; NS = not significant.

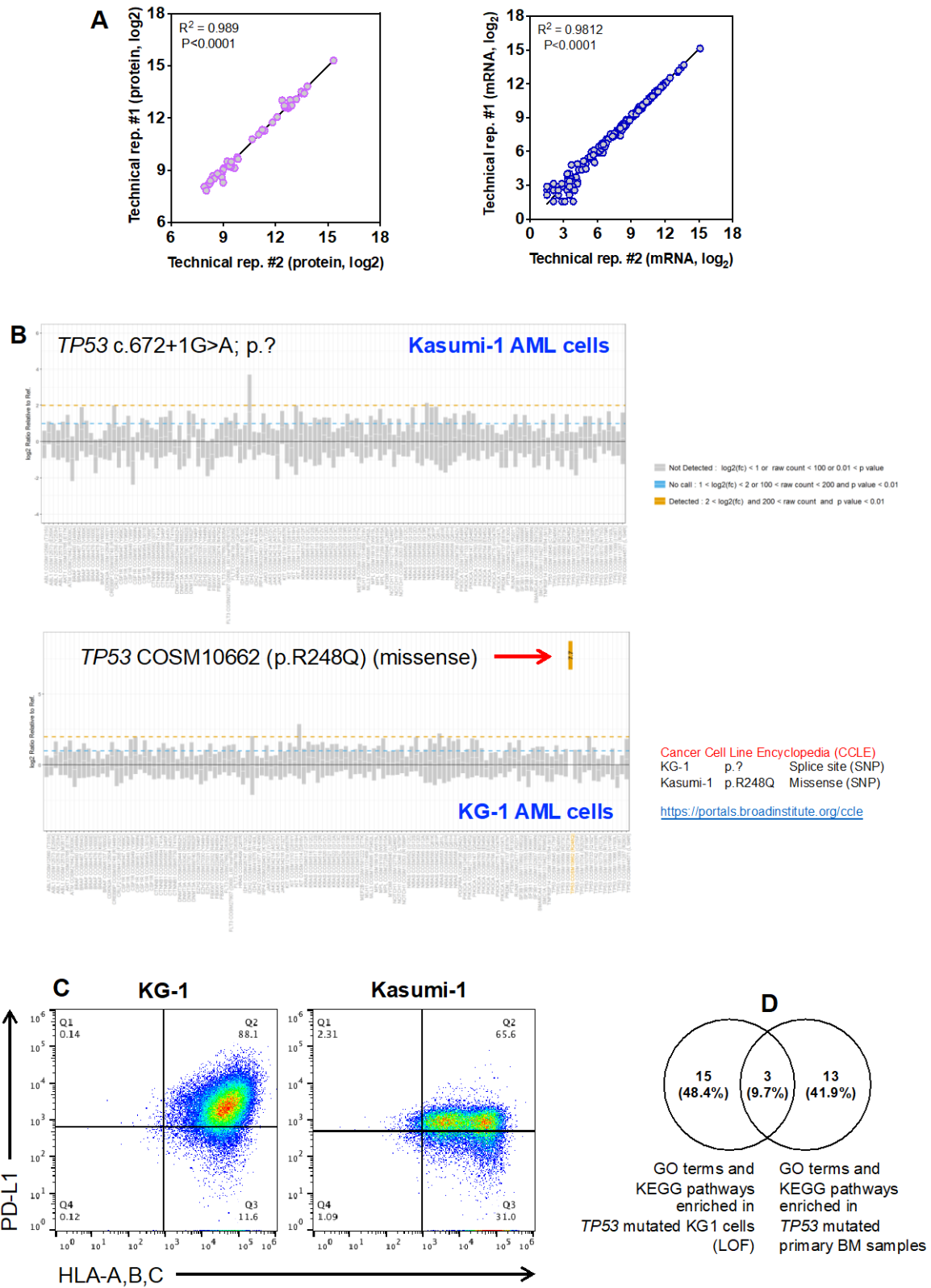


Fig. S6

Supplemental Figure 6: *TP53* status and expression of PD-L1 and human leukocyte antigen (HLA) class I molecules in Kasumi-1 and KG-1 AML cell lines. **A)** Inter-assay reproducibility (replicate 1 and 2) of mRNA and protein measurements with the nCounter Vantage 3D™ Heme assay. R = Spearman correlation coefficient. **B)** Detection of single nucleotide variants (SNV) in KG-1 and Kasumi-1 cells using the nCounter Vantage 3D™ Heme assay (NanoString Technologies; for research use only and not for use in diagnostic procedures). **C)** Flow cytometric detection of PD-L1 and HLA class I molecules in KG-1 and Kasumi-1 cells. Data were visualized using the FlowJo™ software package (version 10.6.1) and are representative of results in three independent experiments. **D)** Venn diagram showing the overlap between GO terms and KEGG pathways captured by the differentially expressed genes between KG-1 and Kasumi-1 AML cells and primary BM samples from patients with *TP53* mutated and *TP53* wild type AML.

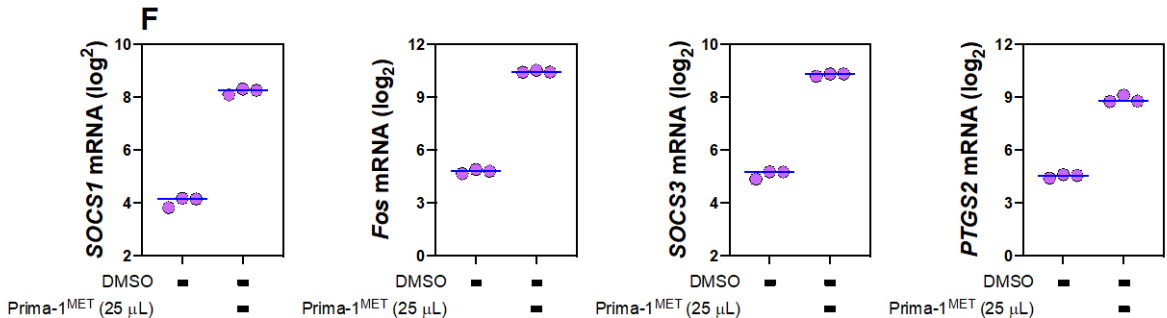
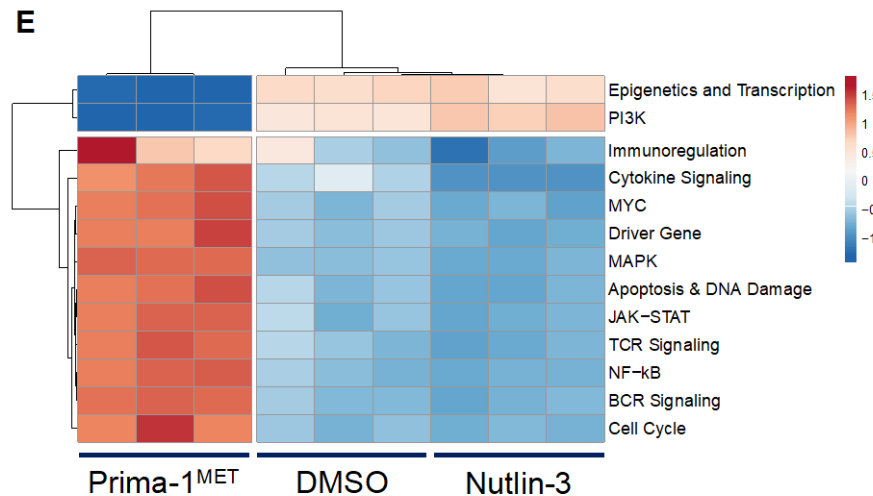
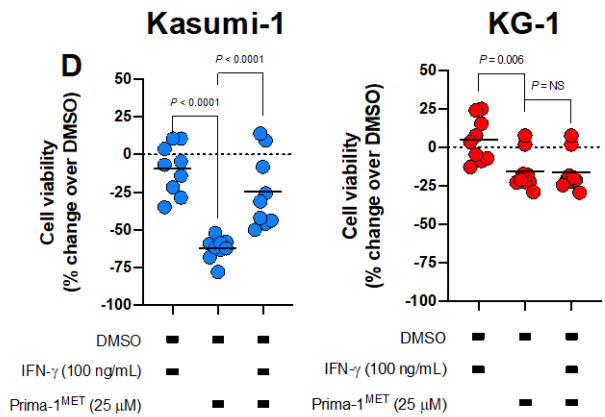
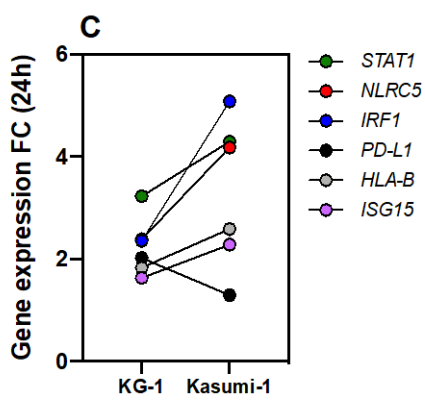
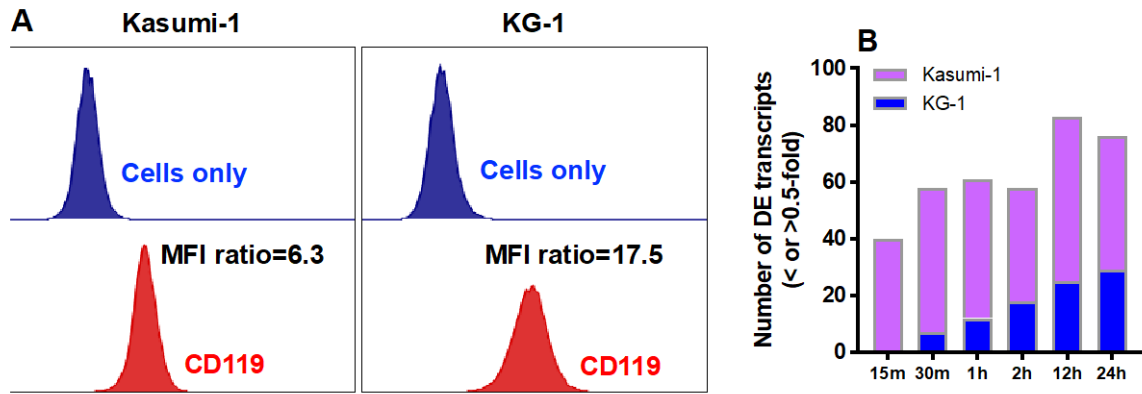


Fig. S7

Supplemental Figure 7: Response to exogenous IFN- γ and TP53 reactivation in KG-1 and Kasumi-1 AML cell lines. **A)** Flow cytometric detection of CD119, the ligand-binding portion of the IFN- γ receptor, in KG-1 and Kasumi-1 cells. Data were visualized using the FlowJo™ software package (version 10.6.1) and are representative of results in three independent experiments. MFI = mean fluorescence intensity. **B)** Number of differentially expressed (DE) transcripts in KG-1 and Kasumi-1 cells after IFN- γ stimulation (100 ng/mL) for up to 24 hours. RNA was extracted and processed as detailed in Materials and Methods. **C)** Fold change (FC) of selected target genes in IFN- γ -stimulated KG-1 and Kasumi-1 cells (24 hours compared with baseline). Each dot represents median gene expression (triplicate measurement; further details in Methods). **D)** KG-1 and Kasumi-1 cells were cultured for 24 hours with IFN- γ , with or without p53 reactivation with induction of massive apoptosis-1 (Prima-1^{MET}; 25 μ M; number of experiments = 9). A non-radioactive, colorimetric assay (MTT; Merck, Darmstadt, Germany) was used to measure cellular metabolic activity as an indicator of cell viability and proliferation. Black bars denote median values. Prima-1^{MET} was dissolved using dimethyl sulfoxide (DMSO). **E)** Kasumi-1 cells were cultured for 24 hours with either Prima-1^{MET} (25 μ M) or nutlin-3 (5 μ M), an MDM2 inhibitor, followed by gene expression analysis (number of experiments = 3). DMSO was used as a control culture condition. Pathway scores were computed as the weighted sum of predefined gene sets, as previously published.² **F)** Transcriptomic changes in Kasumi-1 cells treated with Prima-1^{MET}. The expression of inhibitors of IFN signaling (*SOCS1* and *SOCS3*) and targets for transactivation by TP53 (*FOS* and *PTGS2*) is shown. Number of experiments = 3.

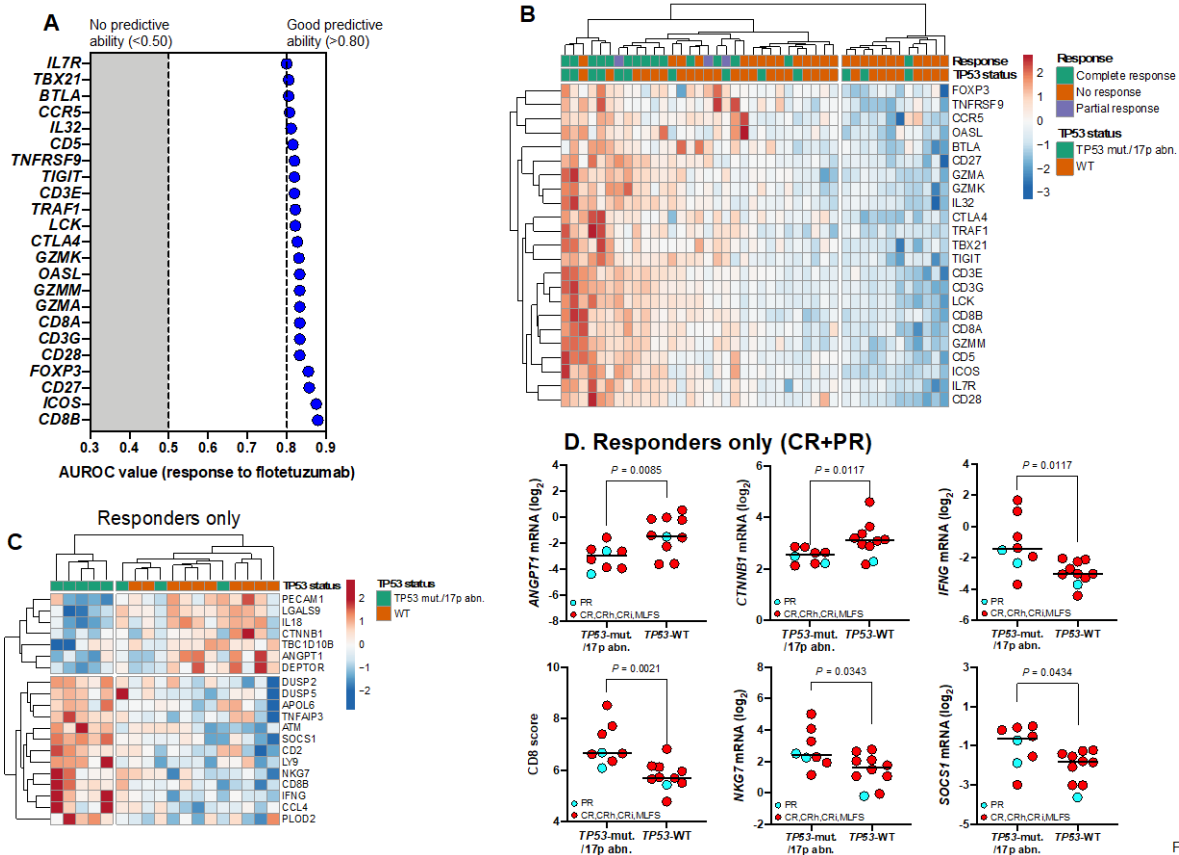


Fig. S8

Supplemental Figure 8: Predictors of response of R/R AML to flotetuzumab. **A)** Top-ranking genes (n=23) associated with complete and partial response to flotetuzumab with an area under the receiver operating characteristics (AUROC) value greater than 0.8. AUROC analyses were performed using the SPSS software package. AUROC=1.0 would denote perfect prediction and AUROC=0.5 would denote no predictive ability. **B)** Heatmap summarizing the expression of the top-ranking 23 genes from **Panel A**. ClustVis, an online tool for clustering of multivariate data, was used for data analysis and visualization.¹⁰ **C)** Top differentially expressed genes between flotetuzumab responders with (n=8) or without (n=10) *TP53* abnormalities. **D)** Expression of potential drivers of immune infiltration and immunotherapeutic benefit in responders with or without *TP53* abnormalities (color-coded by response, either complete [red circles] or partial [cyan circles]). Data were compared using the Mann-Whitney *U* test for unpaired determinations.

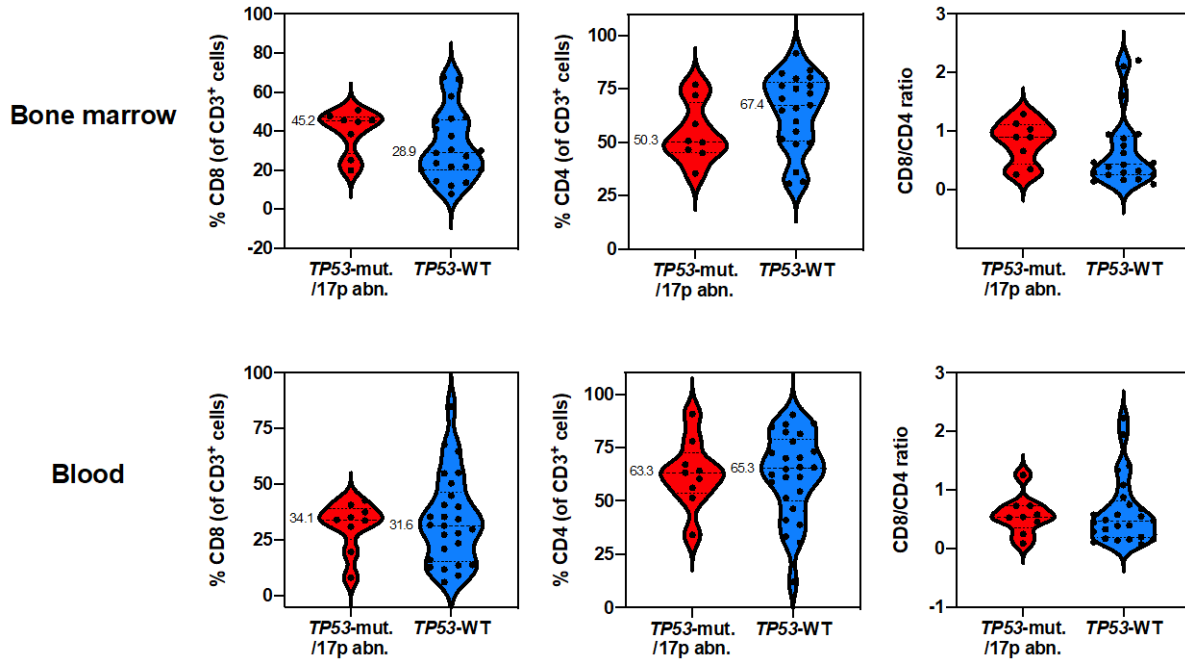


Fig. S9

Supplemental Figure 9: Flow cytometry measurement of CD8⁺ and CD4⁺ T cells in paired blood and bone marrow samples from patients with (n=9) and without *TP53* abnormalities (n=26) on study. Violin plots summarizing the frequency of CD8⁺ and CD4⁺ T cells (of CD3⁺ T cells) and the CD8/CD4 ratio. Median values are shown in the plots. All monoclonal antibodies were purchased from BD Biosciences (San Jose, CA).

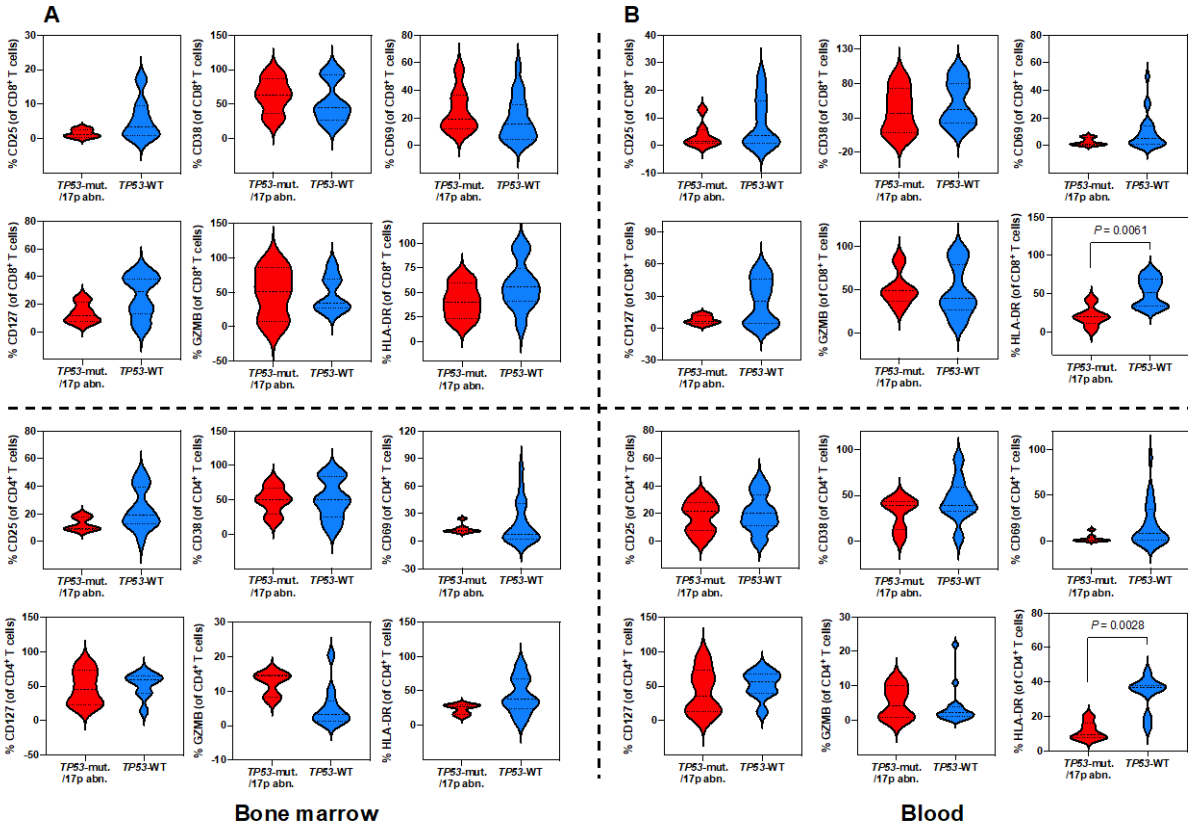


Fig. S10

Supplemental Figure 10: Flow cytometry measurement of activation and cytolytic markers on CD8⁺ and CD4⁺ T cells in paired blood and bone marrow samples from patients with (n=9) and without TP53 abnormalities (n=26) on study. Violin plots summarizing the frequency of CD8⁺ and CD4⁺ T cells co-expressing each marker. All monoclonal antibodies were purchased from BD Biosciences (San Jose, CA). Data were compared with the Mann-Whitney *U* test for unpaired determinations. *P* = NS unless otherwise indicated.

References

1. Wagner S, Vadakekolathu J, Tasian SK, et al. A parsimonious 3-gene signature predicts clinical outcomes in an acute myeloid leukemia multicohort study. *Blood Adv.* 2019;3(8):1330-1346.
2. Vadakekolathu J, Minden MD, Hood T, et al. Immune landscapes predict chemotherapy resistance and immunotherapy response in acute myeloid leukemia. *Sci Transl Med.* 2020;12:eaaz0463.
3. Danaher P, Warren S, Dennis L, et al. Gene expression markers of Tumor Infiltrating Leukocytes. *J Immunother Cancer.* 2017;5:18.
4. Cancer Genome Atlas Research N, Ley TJ, Miller C, et al. Genomic and epigenomic landscapes of adult de novo acute myeloid leukemia. *N Engl J Med.* 2013;368(22):2059-2074.
5. Newman AM, Liu CL, Green MR, et al. Robust enumeration of cell subsets from tissue expression profiles. *Nat Methods.* 2015;12(5):453-457.
6. van Galen P, Hovestadt V, Wadsworth li MH, et al. Single-cell RNA-seq reveals AML hierarchies relevant to disease progression and immunity. *Cell.* 2019;176(6):1265-1281 e1224.
7. Zhou Y, Zhou B, Pache L, et al. Metascape provides a biologist-oriented resource for the analysis of systems-level datasets. *Nat Commun.* 2019;10(1):1523.
8. Subramanian A, Tamayo P, Mootha VK, et al. Gene set enrichment analysis: a knowledge-based approach for interpreting genome-wide expression profiles. *Proc Natl Acad Sci U S A.* 2005;102(43):15545-15550.
9. Cerami E, Gao J, Dogrusoz U, et al. The cBio cancer genomics portal: an open platform for exploring multidimensional cancer genomics data. *Cancer Discov.* 2012;2(5):401-404.
10. Metsalu T, Vilo J. ClustVis: a web tool for visualizing clustering of multivariate data using Principal Component Analysis and heatmap. *Nucleic Acids Res.* 2015;43(W1):W566-570.